Bioinspired Intervertebral Disc with Multidirectional Stiffness Prepared via Multimaterial Additive Manufacturing

Document Version
Accepted author manuscript

[Link to publication record in Manchester Research Explorer](#)

Citing this paper
Please note that where the full-text provided on Manchester Research Explorer is the Author Accepted Manuscript or Proof version this may differ from the final Published version. If citing, it is advised that you check and use the publisher's definitive version.

OPEN ACCESS

Bioinspired Intervertebral Disc with Multidirectional Stiffness Prepared via Multimaterial Additive Manufacturing

Guangsheng Song, Zhihui Qian*, Xiangyu Liu, Boya Chen, Guanghui Li, Zhenguo Wang, Kunyang Wang, Zhenmin Zou, Fabio Galbusera, Marco Domingos, Lei Ren*, Hans-Joachim Wilke and Luquan Ren

G. S. Song, Z. H. Qian, X. Y. Liu, B. Y. Chen, G. H. Li, Z. G. Wang, K. Y. Wang, L. Ren, L. Q. Ren

Key Laboratory of Bionic Engineering, Ministry of Education

Jilin University

Changchun 130022, China

E-mail: *zhqian@jlu.edu.cn*

Z. M. Zou, M. Domingos, L. Ren

Department of Mechanical, Aerospace and Civil Engineering

University of Manchester

Manchester M13 9PL, United Kingdom

E-mail: *lei.ren@manchester.ac.uk*

F. G*albusera*

Spine Center

Schulthess Clinic

Zürich 8008, Switzerland

H. J. Wilke

Institute of Orthopaedic Research and Biomechanics

Ulm University Medical Centre

University of Ulm

Ulm 89081, Germany

Z. H. Qian, L. Ren

Institute of Structured and Architected Materials

Liaoning Academy of Materials

Shenyang 110167, China.

K. Y. Wang, L. Q. Ren

Institute for Bionics Health

Bionic Healthcare Engineering Research Center

Weihai Institute for Bionics, Jilin University

Weihai 264207, Chin*a*

Keywords

Degenerative disc disease (DDD) has become a significant public health issue worldwide. This can result in loss of spinal function affecting patient health and quality of life. Artificial total disc replacement (A-TDR) is an effective approach for treating symptomatic DDD that compensates for lost functionality and helps patients perform daily activities. However, because current A-TDR devices lack the unique structure and material characteristics of natural intervertebral discs (IVDs), they fail to replicate the multidirectional stiffness needed to match physiological motions and characterize anisotropic behavior. It is still unclear how the multidirectional stiffness of the disc is affected by structural parameters and material characteristics. Herein, we develop a bioinspired intervertebral disc (BIVD-L) based on a representative human lumbar segment. The proposed BIVD-L reproduces the multidirectional stiffness needed for the most common physiological kinematic behaviors. The results demonstrate that the multidirectional stiffness of the BIVD-L can be regulated by structural and material parameters. The results of this research deepen knowledge of the biomechanical behavior of the human lumbar disc and may provide new inspirations for the design and fabrication of A-TDR devices for both engineering and functional applications.

1. Introduction

Lower back pain has become a major global health issue, increasing healthcare expenditures and imposing a heavy financial burden on patients.[1-3] Although lower back pain involves multiple factors, and its causes have not been fully explained, it is generally accepted that intervertebral disc (IVD) degeneration is a contributing component.[4] Approaches to treat degenerative IVD include fusion surgery and A-TDR.[5-8] The benefits of A-TDR include restoring the range of motion (ROM) and disc height and relieving pain in patients,[9-12] and thus A-TDR has become a popular alternative to fusion for treating symptomatic DDD.[13-15] A-TDR devices have undergone substantial development and have been used in clinical practice[6, 8, 16-20] around the world since they were proposed in the 1950s.[21] However, these available A-TDR devices generally have a joint structure design (e.g., ball and socket joints,[22] ball and trough joints,[23] and saddle joints[24]) and are composed of a single material (e.g., metal,[7] ceramic,[24] polymer,[25] and composite material[26]), which result in mismatched physiological motions and homogeneous stiffness properties.[11, 27, 28] In contrast, natural IVD demonstrates unrivaled anisotropic mechanical behaviors and excellent performance, which may originate from angle-ply structure and multimaterial composition.[29, 30] To date, creating an A-TDR device with multidirectional stiffness similar to that of natural IVDs is still a challenge in the field, which may be mostly attributed to the incomplete scientific explanation of multidirectional stiffness of natural IVDs in terms of structural and material properties.

To develop an A-TDR device with multidirectional stiffness, we propose a bioinspired intervertebral disc (BIVD-L) device based on the structure and material of natural lumbar IVD. The developed BIVD-L replicates the

heterogeneous structure of fibers and graded features of the lamellae of natural IVDs in contrast to current A-TDR devices. Based on this improvement, the effects of structural parameters and material properties on multidirectional stiffness are explored. The research may provide a new approach for engineering designers, materials scientists, process engineers, or surgeons who are engaged in the development of A-TDR devices.

2. Results and Discussion

2.1. Design Strategy of a BIVD–L with Multidirectional Stiffness
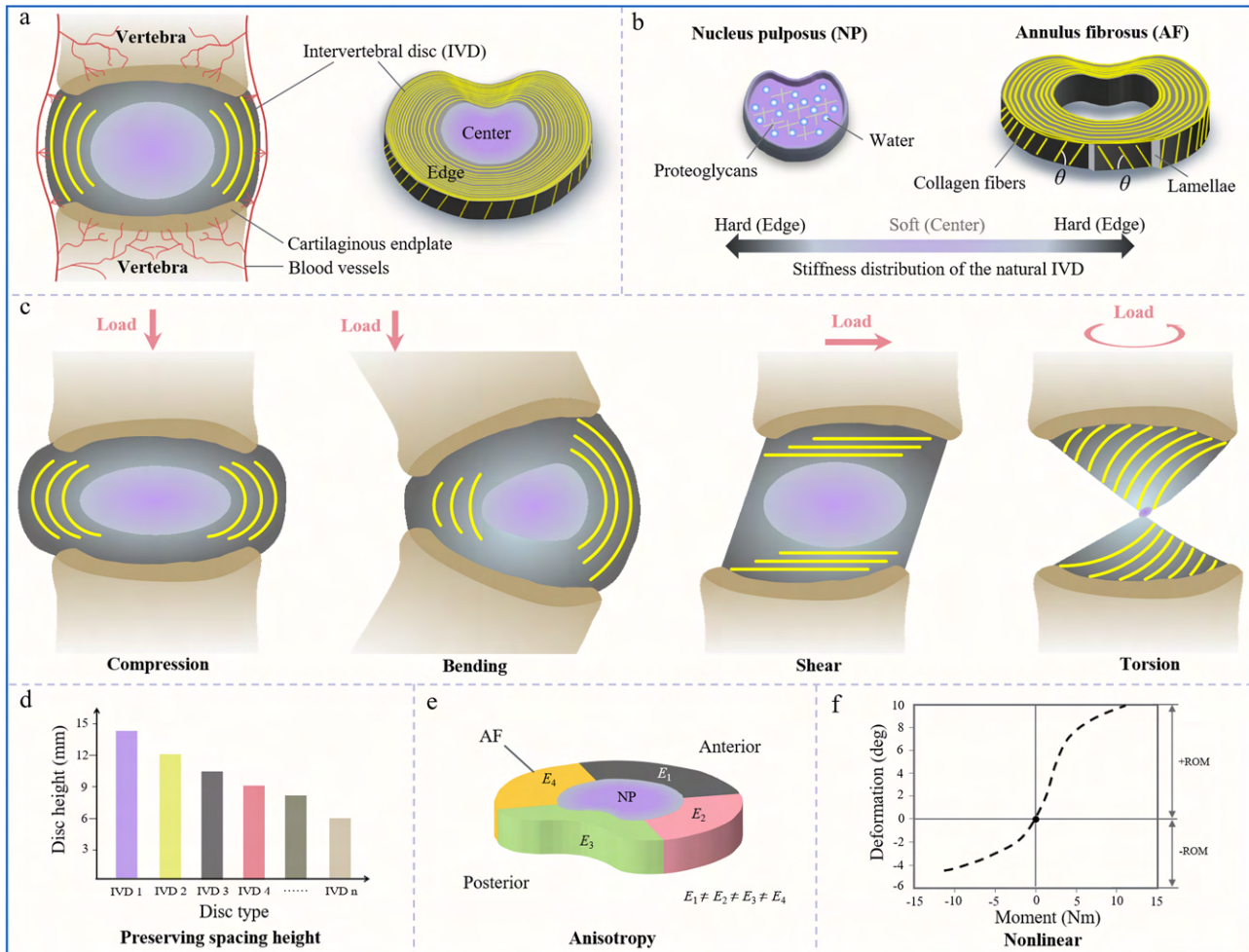

Figure 1. Schematic diagram of biological structures, functionalities, and mechanical properties of natural IVD. a) Structural characteristics of the FSU, including the superior and inferior vertebra, and natural IVD. b) The unique structure and material properties of natural IVD. c) Kinematic behaviors. d) Preservation of disc height. Due to the individual differences in human vertebrae, the disc height is also varied.[31] e) Different mechanical properties due to the unique structure and material of natural IVD. E_1, E_2, E_3, and E_4 indicate the different mechanical properties of the four regions of the annulus fibrosus.[27] f) Nonlinear load–deformation behavior.[32]

Figure 1 demonstrates the biological structure, and functional and mechanical properties of the human functional spinal unit (FSU). As shown in Figure 1a, natural IVD is composed of nucleus pulposus (NP), annulus fibrosus (AF), and cartilaginous endplates.[33-35] Figure 1b shows the microstructure and material composition of NP and AF.[36-38] NP is located in the inner center and is composed of hydrophilic proteoglycans and water. NP is isotropic

and characterized by a good hydrostatic stiffness,[39] which is much less than that of the surrounding AF that consists of type I collagen and proteoglycans. AF consists of collagen fibers and annulus lamellae, and the fibers are embedded in the same lamellae with parallel alignment and are positioned crosswise to one another in the neighboring lamellae.[29] Fibers have complex orientational and distributional features in space. Furthermore, lamellae are functionally graded, and the interior stiffness is less than the exterior stiffness.[40-42] As shown in Figure 1c, due to its unique structure and material composition, natural IVD shows considerable flexibility and enables the FSU to perform kinematic behaviors, e.g., compression, bending, shear and torsion. It also allows preservation of the height of the intervertebral space in compression, as shown in Figure 1d, and is characterized by different mechanical properties (Figure 1e). These different mechanical properties demonstrate that the physiological stiffness of natural IVD is variable (Figure 1f).[43, 44] As a result, the anisotropic mechanical properties are strongly associated with the material and proper structure that replicate the key anatomical features of the NP and AF.
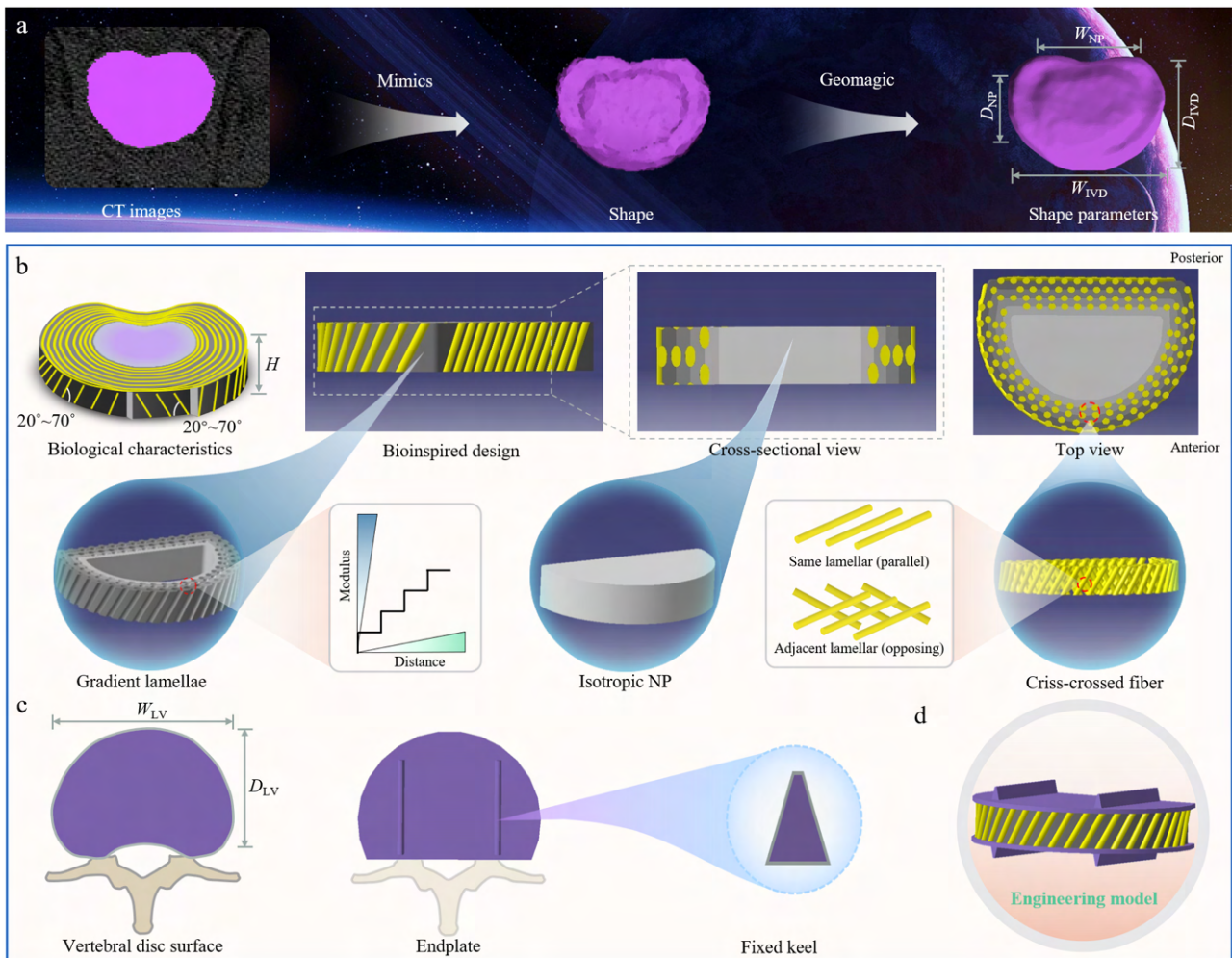
Figure 2. Schematic overview of the BIVD-L structural design examined in this study. a) Morphology and shape parameters are obtained from CT images. b) Bioinspired design is performed on the external morphology and internal features of natural IVD. c) An endplate is designed based on the inferior surface shape of the L4 vertebra, and fixed keels are used to achieve long-term fixation to the upper and lower vertebra. d) A bionic engineering model composed of distinct constructs that mimic the structure of natural IVD.

Inspired by the functionalities and structure of natural IVD, a BIVD-L engineering model that possesses multidirectional stiffness properties is engineered in this study (**Figure 2**). In Figure 2a, the outer shape of natural IVD in the L4-L5 segment is obtained based on computed tomography (CT) (Brilliance iCT 256, Philips, Netherlands) images of a healthy volunteer (age 28 years, height 176 cm, weight 75 kg). Moreover, the outer shape parameters such as the width (W_{IVD}), depth (D_{IVD}), and height of the IVD (H) and the width (W_{NP}) and depth of the NP (D_{NP}) are measured. According to the inner structural characteristics of the natural IVD, a BIVD-L structural model is established by common computer-aided design (CAD) software (CATIA, V5 R20, Dassault Systèmes, France), and the monolithic form is a D-shape that approximates the morphology of natural IVD (Figure 2b). The fibers with angles 20°~70° to the transverse plane are embedded in the same annulus lamellae, and the fibers of the two adjacent lamellae are arranged in a crisscrossed pattern.[45] The proposed BIVD-L structural model mimics the structure of the natural fibers network, and the designed lamellae have graded stiffness for mimicking the graded lamellae, where the stiffness is less on the interior than the exterior. NP with isotropy is placed in the structural center that is surrounded by the AF. The shape of the endplate is also designed, and the dimensions are confirmed based on the size of the inferior surface of the L4 vertebra, such as the width (W_{LV}) and depth (D_{LV}) of the lower vertebra. Keels are designed and used to achieve immediate fixation with the superior and inferior adjacent vertebra (Figure 2c). The final integrated BIVD-L engineering model comprised of the inner NP, the outer AF, and the superior and inferior endplates is then generated (Figure 2d). The detailed dimensions of the BIVD-L are designed and listed in Figure S1 and Table S1 in the Supporting Information (details provided in Section S1, Supporting Information).

2.2. Material Properties and Manufacturing Processes

Polymer materials, especially functionally graded materials (FGMs), have been used for a wide range of applications in contemporary interdisciplinary fields such as biomedical implants.[46-49] In this study, advanced polymer materials with various Shore hardness values are employed to fabricate a BIVD-L based on the structural design and dimensional parameters shown in **Figure 3**a. The softer Agilus30[TM] FLX 935 (Stratasys Ltd., Eden Prairie, MN, USA) can be mixed with the harder VeroBlackPlus[TM] RGD 875 (Stratasys Ltd., Eden Prairie, MN, USA) in various proportions. VeroPureWhite[TM] RGD 837 (Stratasys Ltd., Eden Prairie, MN, USA) has a stiffness similar to that of bone and is generally used to manufacture rigid components. The material biocompatibility was assessed *in vitro* by culturing murine osteoblastic MC3T3 cells using a CCK-8 assay (details provided in Section S2, Supporting Information). The experimental results indicated that the selected material has mild or slight cytotoxicity. Material mechanical tests are carried out using a universal tensile testing machine (KQL computer-controlled electronic universal testing machine, China) as shown in Figure S3 in the Supporting Information (details provided in Section S3, Supplementary Information). These results showed that the addition of VeroBlackPlus[TM] RGD 875 increases the stiffness of the specimens (Figure 3b) and enables the preparation of stiffness-graded structures. This offers an approach to approximating the soft and hard distributions of natural IVD. Therefore, Agilus 30[TM] FLX 935 is chosen as the NP component, FLX 9895 is utilized to fabricate the fiber component, the material with different Shore

hardness values from FLX 9840 to FLX 9895 is chosen as the material to create a graded lamella, and VeroPureWhite[TM] RGD 837 is used to manufacture an endplate with sufficient strength.
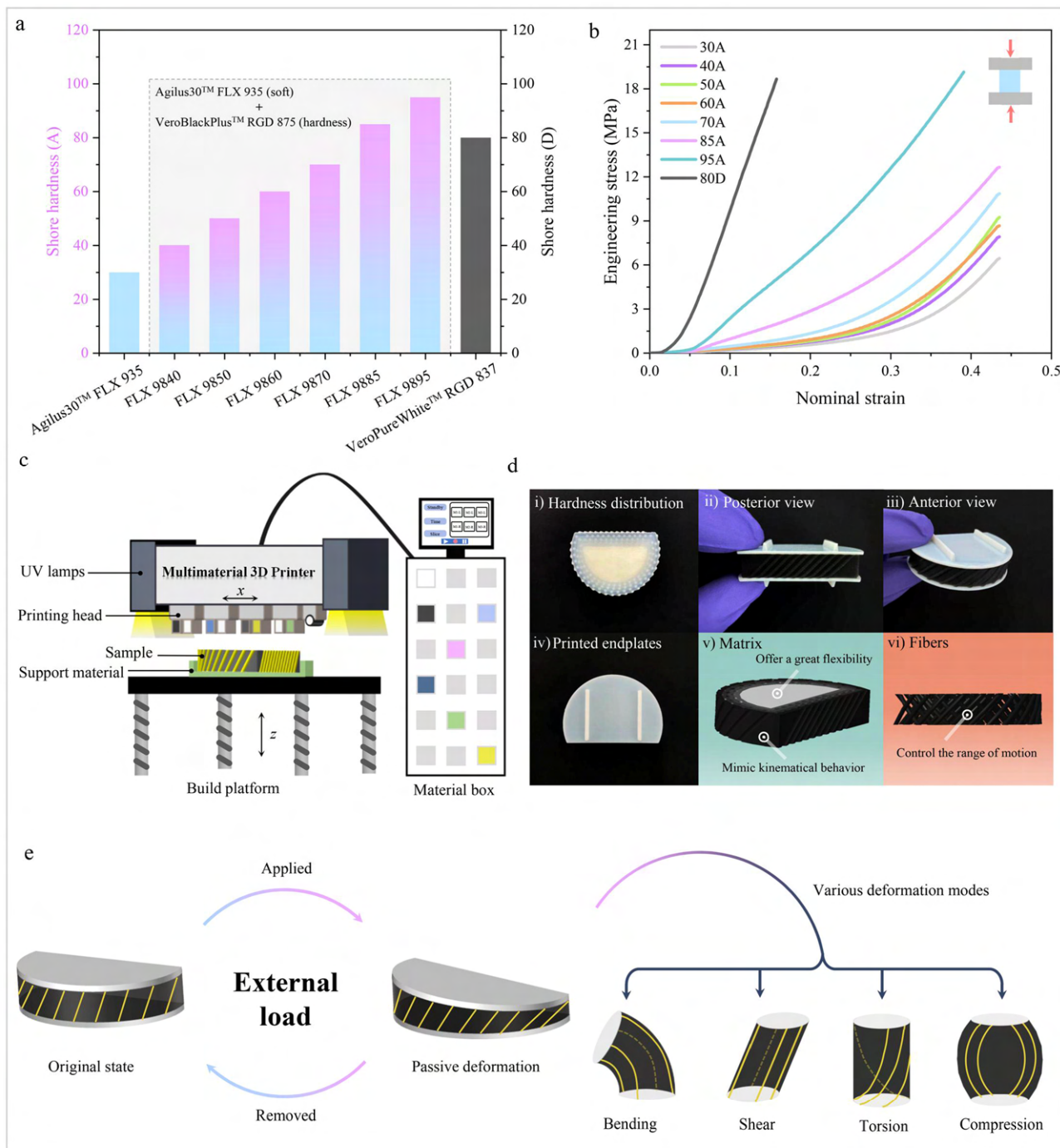

Figure 3. Material properties, multimaterial fabrication platform and various deformation modes. a) Plot comparing the Shore hardness values of Agilus30[TM] FLX 935, VeroPureWhite[TM] RGD 837, and various other materials. b) Stress–strain graph showing the mechanical behavior of materials with Shore hardness values of the Agilus30[TM] FLX 935, VeroPureWhite[TM] RGD 837, and blends of materials of different Shore hardness values. c) Illustration of the fabrication of an engineering model by the Polyjet multimaterial 3D printer. d) The BIVD-L reproduces the structural and graded characteristics of natural IVD. e) Schematics of the BIVD-L deformation.

Multimaterial additive manufacturing (MM-AM)[50-52] technology provides a novel opportunity for fabricating

the complex heterogeneous fiber structure and the graded lamellae design employed in this study. To evaluate the BIVD-L mechanical properties, we fabricated the BIVD-L using a commercial multimaterial 3D printer (Stratasys PolyJet 850, Stratasys Ltd., Eden Prairie, MN, USA). We translated this engineering model into an instantiated physical prototype as shown in Figure 3c (details provided in Section S4, Supporting Information). As shown in Figure 3d, we printed a prototype BIVD-L based on the dimensions listed in Table S1 (details provided in Section S1, Supporting Information), achieving a mass of approximately 210 g. The printed BIVD-L replicates the structural and material characteristics of natural IVD (details provided in Movie S1, Supporting Information). Furthermore, due to its extraordinary structural and material properties, the BIVD-L can deform and recover under different conditions and exhibits great multidirectional stiffness (Figure 3e).

2.3. Multidirectional Stiffness Experiment

To verify the multidirectional stiffness of the BIVD-L, a test apparatus was established using a robotic system, as shown in **Figure 4a**. A schematic diagram of the test apparatus, the three-dimensional coordinate system, three-dimensional motion and primary loading direction, and test conditions are shown in Figure 4b-d, respectively (details provided in Section S5, Supporting Information).

As shown in Figure 4e, an experiment was performed to assess whether the BIVD-L had multidirectional stiffness based on typical spine behaviors (details provided in Movie S2, Supporting Information). The corresponding load–deformation curve is shown in Figure 4f and indicates a nonlinear relationship between the input load and output displacement. For left lateral bending, the maximum angle was -8.07° when the moment reached -7.5 Nm, but the maximum angle was 6.17° when the moment reached 7.5 Nm for right lateral bending. The results illustrated that the left bending stiffness was less than the right bending stiffness. In the flexed state, the BIVD-L could bend to 6.66° under a load of 7.5 Nm, and it could bend to -6.1° under a load of -7.5 Nm in the extended state. The outcome meant that the stiffness in flexion was less than the stiffness in extension. In the left rotation state, the BIVD-L could bend to 6.08° under a load of 7.5 Nm, and it could bend to -7.09° under a load of -7.5 Nm in the right rotation state. The results demonstrated that the stiffness was greater in the left rotation than the right rotation. In axial compression, the maximum displacement was -6.43 mm when the compressive force reached -280 N. Figure 4f showed that the angle or displacement significantly differed with increasing magnitude of moment or force, and the angle of rotation and displacement differed under the condition of equal moment or force. The above analysis highlights that the stiffness under typical kinematical behavior varied from one case to another, which demonstrated that the BIVD-L possessed multidirectional stiffness. In fact, compared to an A-TDR device composed of a homogeneous material exhibiting almost equal stiffness under different loading conditions,[11] our results primarily showed that the BIVD-L with its angle-ply structure and multimaterial composition successfully reproduced nonlinear mechanical properties similar to those of natural IVD by mimicking the typical

three-dimensional motions of the human FSU. Encouragingly, the load–displacement curve of the BIVD-L is similar to that of the natural IVD reported in related literature[43, 44]. To assess effects of the integration and stability of the BIVD-L with the artificial vertebrae, the BIVD-L was subjected to a fatigue load test (details provided in Section S6, Supporting Information). This fatigue results demonstrated that the BIVD-L remained the integration and stability with the artificial vertebrae after 100,000 cycles. Furthermore, this advanced investigation of how several intralamellar parameters, such as orientation angle, lamellar hardness and disc height, affect multidirectional stiffness plays a significant role in deepening the understanding of anisotropic mechanical properties of natural IVD.
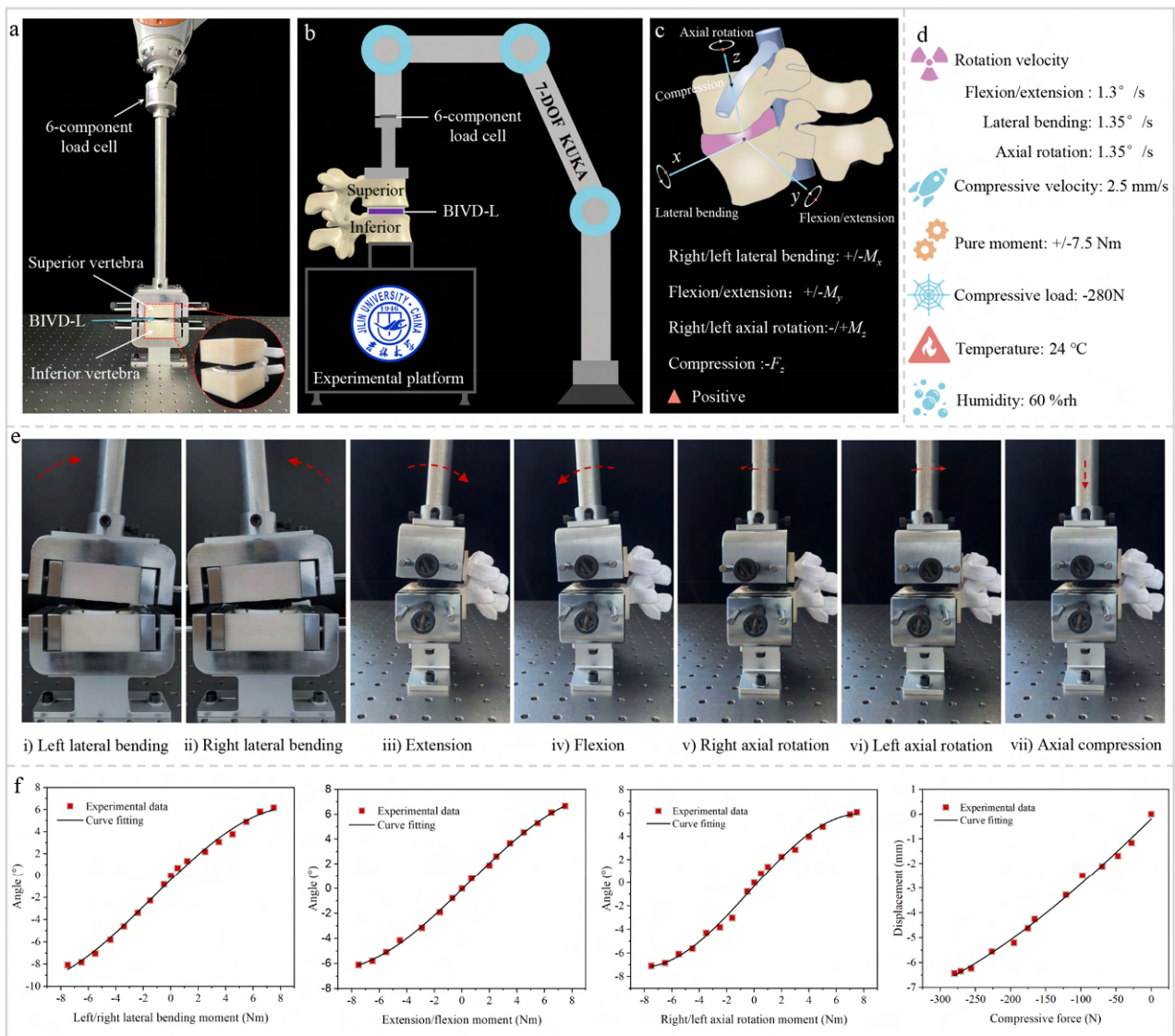

Figure 4. Experimental validation of multidirectional stiffness. a) The test apparatus included a KUKA robotic system, a 6-component load cell, fixture, a BIVD-L and an experimental platform. b) Schematic diagram of the multidirectional stiffness test. c) Definition of the three-dimensional coordinate system and definition of the direction of three-dimensional motion. d) Test conditions. e) Multidirectional stiffness was tested by mimicking the typical spine kinematic behaviors. f) Typical load–displacement curve.

2.4. Mechanism Analysis of Multidirectional Stiffness

To further investigate the mechanism underlying multidirectional stiffness, we designed and fabricated several samples with different fiber orientation angle, lamellar hardness, and disc height. Detailed images of the different BIVD-L samples are listed in Figure S6 in the Supporting Information (details provided in Section S7, Supporting Information). The mechanism underlying multidirectional stiffness was analyzed under the same experimental platform, conditions, and protocol as described in Section S5 in the Supporting Information. In previous studies, Heuer et al.[43] reported the physiological ROM of natural lumbar IVD for intact human cadavers subjected to ± 7.5 Nm moment in extension/flexion, right lateral bending, and left axial rotation. Wilke et al.,[53] and Hitchon et al.,[54] determined the physiological ROM for left/right lateral bending, extension/flexion, and right/left axial rotation by natural lumbar IVD of intact human cadavers under ± 7.5 Nm, and ± 6 Nm moment, respectively. Shikinami et al.[55] obtained the physiological ROM data under a 900 N compressive force with whole lumbar specimens from fresh human cadavers. In this study, these intact human cadaver data were regarded as natural IVD group.

Figure 5 shows that all the curves exhibit obvious nonlinear characteristics. In particular, Figure 5 shows the discrepancy of multidirectional stiffness in a typical kinematic pattern. Figure 5a demonstrates that multidirectional stiffness can be controlled by regulating the angle of orientation of fibers. Compared to the 45° orientation angle, the stiffness of the orientation angle of 30° decreased, and the stiffness of the orientation angle of 60° increased. This result illustrated that a decrease or increase in stiffness in a certain direction can be controlled by changing the fiber orientation angle. The optimal fiber orientation angle was found to be 60°, which is similar to that of the natural IVD. For 30° or 45° fibers, some of the ROM values are similar to those of the natural IVD. Clearly, our experimental results are either similar to or different from those of the natural IVD determined by Wilke et al.[53] and Shikinami et al.[55]. In contrast, the experimental results were in approximate agreement with natural IVD data from intact human cadavers reported by Heuer et al.[43] and Hitchon et al.[54] This comparison with the natural IVD showed that the fiber orientation angle in the center of natural IVD was relatively small, and thus it showed better flexibility and was larger at the edge than at the center to show great rigidity. The results illustrated that the fiber orientation angle had beneficial influences on multidirectional stiffness and revealed that the fiber orientation angle of natural IVD gradually increased from the inner center to the outer edge regardless of whether there were certain discrepancies between our results and natural IVD data. This key finding deepens our understanding of how the fiber orientation angle affects the anisotropy of natural IVD, and in particular provides a strong experimental support for the establishment of appropriate theoretical and physical modeling.

Figure 5b provides evidence that lamellar hardness may be adjusted to control multidirectional stiffness. The stiffness decreased for some specimens with certain hardness values (40A, 50A, 60A, 70A) and increased for other specimens with certain hardness values (60A, 70A, 85A,95A). This result illustrated that a decrease or increase in stiffness in a certain direction can be controlled by altering the hardness of the lamellae. Compared to those of the natural IVDs, the optimal lamellae are hardness values (60A, 70A, 85A, 95A). The partial ROM for hardness values (40A, 50A, 60A, 70A) and (50A, 60A, 70A, 85A) is also similar to that of the natural IVD. From Figure 5b, we can

observe certain similarities and disparities in with the data from natural IVDs of intact human cadavers.[43, 53-55] This comparison with the natural IVD illustrates that the hardness in the center of the natural IVD is relatively small, so it can undergo a greater deformation, then gradually increases closer to the edge, producing smaller deformations radially. Although there are certain differences from natural IVD data, a key finding for this disparity proved that the anatomical stiffness of natural IVD can be matched by regulating the hardness of the lamellae, which demonstrated that, with reference to our experimental results, the annulus lamellae of natural IVD of the human spine actually has a graded structure from the inner to the outer lamellae, and highlighted the potential of mechanical grading as a way to control multidirectional stiffness.

Figure 5c demonstrates that there was less stiffness for the disc height of 8 mm than 10 mm and more stiffness for the disc height of 12 mm. These results illustrated that a decrease or increase in stiffness in a certain direction can be controlled by regulating the disc height. The optimal disc height was 8 mm, which is similar to that of the natural IVD. The partial ROM values for heights of 10 mm and 12 mm are also similar to those of the natural IVD. Apparently, our experimental results for lateral bending and axial rotational motions showed that natural IVD was higher at the center than the edge, while the flexion and extension results indicated that the anterior was higher than the posterior, and the axial compression results indicated that the overall height of natural IVD was less, in agreement with the morphological height of natural IVD.[56] The discrepancy with the data from natural IVDs showed that the natural disc height is more variable than that revealed in our experimental data, emphasizing the approach to achieve multidirectional stiffness by adjusting the disc height. This supports the potential role of disc height in explaining the anisotropic mechanical properties of natural IVDs.

Little is known in general about the anisotropic mechanical properties of natural IVD. Although the anisotropic mechanical behavior was explored only in terms of fiber orientation in a previous finite element simulation study,[57] our research reveals a key finding that the multidirectional stiffness can be controlled by regulating the fiber orientation angle, lamellar hardness and disc height. To our knowledge, no BIVD-L with multidirectional stiffness based on bionic and MM-AM technology has previously been reported or investigated, and the mechanism for the multidirectional stiffness of natural IVD has not previously been analyzed. This finding demonstrates how heterogeneous structure and mulitimaterial properties can regulate the anisotropic mechanical properties of natural IVD, providing crucial insights into the relationships between the unique structure, function and performance of their complex native tissue. Despite the successful demonstration of the multidirectional stiffness and mechanism of the BIVD-L using an established test apparatus with a robotic system, it is apparent limitations that some ligaments and facet joints which affect the mechanical properties of the FSU were not considered. Compared to experimental results, the finite element prediction results reported were approximate to the data of natural IVD. This result showed that ligaments complex and facet joints could affect the mechanical properties. Meanwhile, the biocompatibility *in vivo* and regeneration were not yet taken into account in this study. The biocompatibility

experiments *in vivo* are helpful to eliminate the interference of other factors and can fully reflect the clinical transformation prospect. In the future, we will explore biocompatibility *in vivo* and tissue repair and regeneration associated with natural IVD [58-60] and monitor tissue rehabilitation after discectomy.[61]
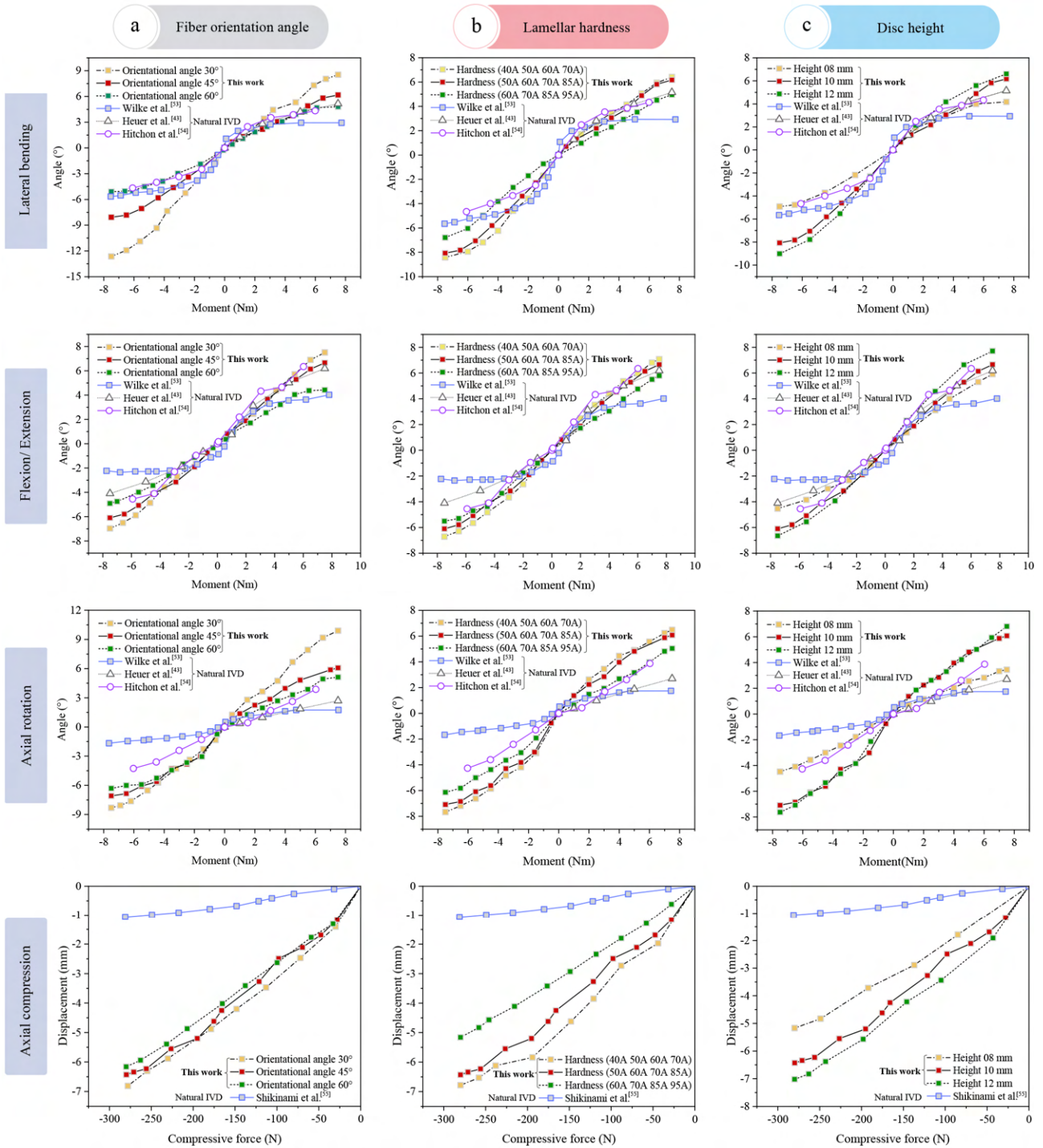

Figure 5. Effect of fiber orientation angle, lamellar hardness, and disc height on multidirectional stiffness and comparisons with data from natural IVDs in the literature. a) Effect of fiber orientation angle on stiffness for the artificial and natural IVDs. b) Effect of lamellar hardness on stiffness for the artificial and natural IVDs. c) Effect of disc height on stiffness for the artificial and natural IVDs.

3. Conclusion

We proposed an approach for an A-TDR implant design using bionic technology to reproduce the unique structure and material properties of natural IVD with excellent mechanical properties. The proposed BIVD-L was fabricated using a multimaterial 3D printer. The proposed BIVD-L with angle-ply structure and multimaterial composition mimics the multidirectional stiffness and mechanical functionality of natural IVD. We also demonstrated that multidirectional stiffness can be controlled by modulating in fine-scale structural parameters such as fiber orientation angle, annular lamellae hardness, and disc height. This approach using multimaterial composition and heterogeneous structure is expected to be applicable to making different TDR implants with multifunctionality, good performance and excellent mechanical functionality superior to that of homogeneous implants. There are still some major challenges to understanding the evolution of anisotropic behavior in a comprehensive way due to the physiological complexity and individual differences of natural IVD. This study offers a scientific explanation of anisotropic behavior in natural IVD and marks a significant advance in our understanding of the relationships between the angle-ply structure, multimaterial composition and anisotropic behavior of the human spine disc. The results of this study may also provide a rational approach for the design of the next generation of A-TDR implants to replace current A-TDR devices, supply technical support for the expansion of the functional range and the improvement of their mechanical properties, and bring new insight and inspiration to researchers and surgeons engaged in applications of A-TDR.

Supporting Information

Supplementary material

Supplementary movie 1

Supplementary movie 2

Ethics Statement

The studies involving human participants were reviewed and approved by the Ethics Committee of the Second Hospital of Jilin University (No. 2021003). The participants provided their written informed consent to participate in this study.

Acknowledgement

Conflict of Interest

The authors declare no conflicts of interest.

References

[1]   C. J. Murray, A. D. Lopez, *N Engl J Med* **2013**, *369*, 448.

[2]   G. B. Andersson, *Lancet* **1999**, *354*, 581.

[3]   B. I. Martin, R. A. Deyo, S. K. Mirza, J. A. Turner, B. A. Comstock, W. Hollingworth, S. D. Sullivan, *JAMA* **2008**, *299*, 656.

[4]   E. J. Carragee, *N Engl J Med* **2005**, *352*, 1891.

[5]   M. Szpalski, R. Gunzburg, M. Mayer, *Eur Spine J* **2002**, *11*, S65.

[6]   C. Schätz, K. Ritter-Lang, L. Gössel, N. Dreßler, *Int J Spine Surg* **2015**, *9*, 1.

[7]   R. C. Sasso, D. M. Foulk, M. Hahn, *Spine* **2008**, *22*, 123.

[8]   M. F. Gornet, J. K. Burkus, R. F. Dryer, J. H. Peloza, *Spine* **2011**, *36*, E1600.

[9]   P. C. McAfee, B. Cunningham, G. Holsapple, K. Adams, S. Blumenthal, R. D. Guyer, A. Dmietriev, J. H. Maxwell, J. J. Regan, J. Isaza, *Spine* **2005**, *30*, 1576.

[10]   J. J. Yue, R. Garcia, Jr., L. E. Miller, *Med Devices (Auckl)* **2016**, *9*, 75.

[11]   C. K. Lee, V. K. Goel, *Spine J* **2004**, *4*, S209.

[12]   B. H. Cummins, J. T. Robertson, S. S. Gill, *J Neurosurg* **1998**, *88*, 943.

[13]   J. Beaurain, P. Bernard, T. Dufour, J. M. Fuentes, I. Hovorka, J. Huppert, J. P. Steib, J. M. Vital, L. Aubourg, T. Vila, *Eur Spine J* **2009**, *18*, 841.

[14]   D. McNally, J. Naylor, S. Johnson, *Eur Spine J* **2012**, *21*, 612.

[15]   J. Lou, Y. Li, B. Wang, Y. Meng, T. Wu, H. Liu, *Medicine* **2017**, *96*, e8291.

[16]   L. Pimenta, R. Springmuller, C. K. Lee, L. Oliveira, S. E. Roth, W. F. Ogilvie, *SAS Journal* **2010**, *4*, 16.

[17]   H. M. Mayer, K. Wiechert, A. Korge, I. Qose, *Eur Spine J* **2002**, *11*, S124.

[18]   J. Y. Lazennec, J. P. Rakover, M. A. Rousseau, *Spine J* **2019**, *19*, 218.

[19]   G. Pokorny, L. Marchi, R. Amaral, R. Jensen, L. Pimenta, *World Neurosurg* **2019**, *122*, e325.

[20]   J. Alex Sielatycki, C. J. Devin, J. Pennings, M. Koscielski, T. Metcalf, K. R. Archer, R. Dunn, S. Craig Humphreys, S. Hodges, *The Spine Journal* **2021**, *21*, 829.

[21]   U. Fernstrom, *Acta Chir Scand Suppl* **1966**, *357*, 154.

[22]   R. B. Delamarter, D. M. Fribourg, L. E. A. Kanim, H. Bae, *Spine* **2003**, *28*, S167.

[23]   M. F. Gornet, J. K. Burkus, M. E. Shaffrey, P. J. Argires, H. Nian, F. E. Harrell, *J Neurosurg: Spine* **2015**, *23*, 558.

[24]   M. A. Finn, D. S. Brodke, M. Daubs, A. Patel, K. N. Bachus, *Eur Spine J* **2009**, *18*, 1520.

[25]   T. K. Daftari, S. R. Chinthakunta, A. Ingalhalikar, M. Gudipally, M. Hussain, S. Khalil, *Clin Biomech* **2012**, *27*, 759.

[26]   H. D. Link, *Eur Spine J* **2002**, *11*, S98.

[27]   Z. Yu, K. Shea, T. Stanković, *J Mech Design* **2019**, *141*, 101406.

[28]   F. Galbusera, C. M. Bellini, T. Zweig, S. Ferguson, M. T. Raimondi, C. Lamartina, M. Brayda-Bruno, M. Fornari, *Eur Spine J* **2008**, *17*, 1635.

[29]   N. L. Nerurkar, D. M. Elliott, R. L. Mauck, *J Biomech* **2010**, *43*, 1017.

[30]   D. M. Elliott, L. A. Setton, *J Biomech Eng* **2000**, *123*, 256.

[31]   M. F. Eijkelkamp, C. C. van Donkelaar, A. G. Veldhuizen, J. R. van Horn, J. M. Huyghe, G. J. Verkerke, *Int J Artif Organs* **2001**, *24*, 311.

[32]   P. A. Halverson, A. E. Bowden, L. L. Howell, *Int J Spine Surg* **2012**, *6*, 78.

[33]   J. C. Iatridis, *Nat Mater* **2009**, *8*, 923.

[34]   E. Siebert, H. Prüss, R. Klinǵebiel, V. Failli, K. M. Einhäupl, J. M. Schwab, *Nat Rev Neurol* **2009**, *5*, 392.

[35]   Y. C. Huanǵ, J. P. Urban, K. D. Luk, *Nat Rev Rheumatol* **2014**, *10*, 561.

[36]   M. May, *Nature* **2013**, *503*, S7.

[37]   F. Han, Q. Yu, G. Chu, J. Li, Z. Zhu, Z. Tu, C. Liu, W. Zhang, R. Zhao, H. Mao, F. Han, B. Li, *Adv Healthc Mater* **2022**, *11*, 2200895.

[38]   A. J. Vernengo, S. Grad, D. Eglin, M. Alini, Z. Li, *Adv Funct Mater* **2020**, *30*, 1909044.

[39]   N. L. Nerurkar, S. Sen, A. H. Huang, D. M. Elliott, R. L. Mauck, *Spine* **2010**, *35*, 867.

[40]   J. J. Cassidy, A. Hiltner, E. Baer, *Connect Tissue Res* **1989**, *23*, 75.

[41]   M. Bhattacharjee, S. Chameettachal, S. Pahwa, A. R. Ray, S. Ghosh, *ACS Appl Mater Interfaces* **2014**, *6*, 183.

[42]   G. Marini, S. J. Ferguson, *Ann Biomed Eng* **2014**, *42*, 1760.

[43]   F. Heuer, H. Schmidt, Z. Klezl, L. Claes, H. J. Wilke, *J Biomech* **2007**, *40*, 271.

[44]   W. T. Edwards, W. C. Hayes, I. Posner, A. A. White, III, R. W. Mann, *J Biomech Eng* **1987**, *109*, 35.

[45]   E. W. Hsu, L. A. Setton, *Magn Reson Med* **1999**, *41*, 992.

[46]   J. Chen, X. Liu, Y. Tian, W. Zhu, C. Yan, Y. Shi, L. B. Kong, H. J. Qi, K. Zhou, *Adv Mater* **2021**, *34*, 2102877.

[47]   L. Y. Zhou, J. Fu, Y. He, *Adv Funct Mater* **2020**, *30*, 2000187.

[48]   M. Naebe, K. Shirvanimoghaddam, *Appl Mater Today* **2016**, *5*, 223.

[49]   Z. Yu, B. Voumard, K. Shea, T. Stanković, *Mater Design* **2021**, *210*, 110046.

[50]   A. Bandyopadhyay, B. Heer, *Mat Sci Eng R* **2018**, *129*, 1.

[51]   P. A. G. S. Giachini, S. S. Gupta, W. Wang, D. Wood, M. Yunusa, E. Baharlou, M. Sitti, A. Menges, *Sci Adv* **2020**, *6*, eaay0929.

[52]   R. S. H. Smith, C. Bader, S. Sharma, D. Kolb, T. C. Tang, A. Hosny, F. Moser, J. C. Weaver, C. A. Voigt, N. Oxman, *Adv Funct Mater* **2019**, *30*, 1907401.

[53]   H. J. Wilke, H. Schmidt, K. Werner, W. Schmölz, J. Drumm, *Spine* **2006**, *31*, 2790.

[54]   P. W. Hitchon, K. Eichholz, C. Barry, P. Rubenbauer, A. Ingalhalikar, S. Nakamura, K. Follett, T. H. Lim, J. Torner, *J Neurosurg: Spine* **2005**, *2*, 339.

[55]   Y. Shikinami, Y. Kotani, B. W. Cunningham, K. Abumi, K. Kaneda, *Adv Funct Mater* **2004**, *14*, 1039.

[56]   H. Schmidt, F. Galbusera, A. Rohlmann, A. Shirazi-Adl, *J Biomech* **2013**, *46*, 2342.

[57]   A. Malandrino, J. Noailly, D. Lacroix, *Comput Methods Biomech Biomed Engin* **2013**, *16*, 923.

[58]   D. Wu, G. Li, X. Zhou, W. Zhang, H. Liang, R. Luo, K. Wang, X. Feng, Y. Song, C. Yang, *Adv Funct Mater* **2022**, *32*, 2209471.

[59]   B. K. Bhunia, S. Dey, A. Bandyopadhyay, B. B. Mandal, *Appl Mater Today* **2021**, *23*, 101031.

[60]   C. Lu, X. Huang, H. Yan, Y. Wang, Y. Wang, S. Zhuo, C. Wei, H. Qiu, X. Yang, Y. Zhang, M. Liu, W. Lei, *Small Struct* **2023**, *4*.

[61]   Y. Shi, K. Wang, X. Feng, S. Li, H. liang, G. Li, W. Li, W. Ke, A. Chen, X. Yang, L. Yang, C. Yan, B. Su, C. Yang, *Nano Energy* **2022**, *96*, 107113.

Table of Contents (TOC)
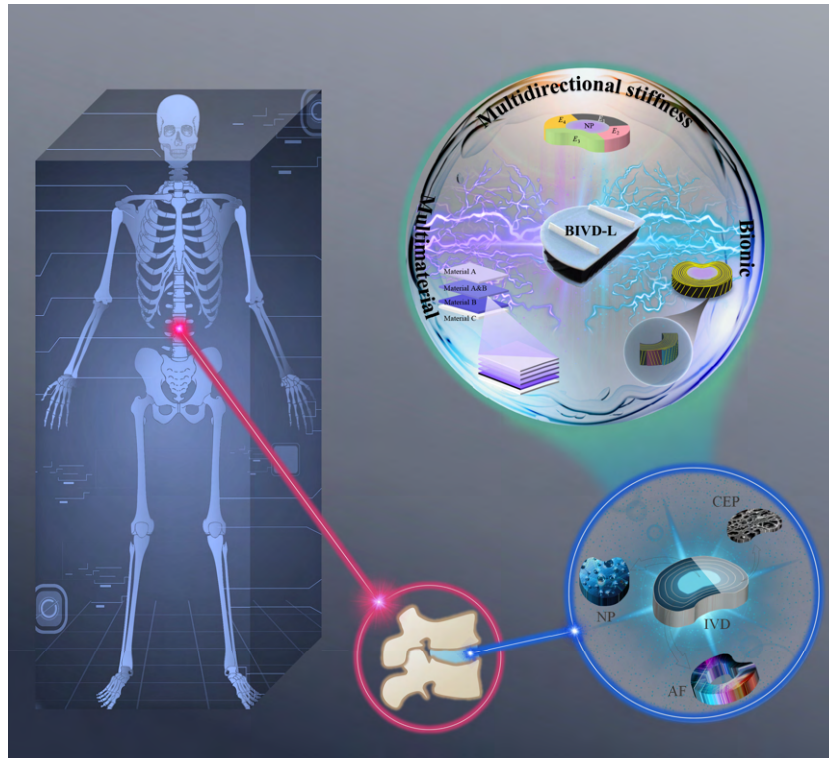
A bioinspired intervertebral disc (BIVD-L) with a heterogeneous fiber structure and graded lamella characteristics based on multimaterial properties and bionic technology is proposed in this research. The proposed BIVD-L reproduces the multidirectional stiffness of the natural IVD and further explains the mechanisms underlying multidirectional stiffness. The proposed BIVD-L demonstrates potential advantages for the development of biomedical devices.